Journal of Bone and Mineral Metabolism (2019) 37:741–748
https://doi.org/10.1007/s00774-018-0976-2

ORIGINAL ARTICLE

# Bone microstructure is significantly altered in CRPS-affected distal tibiae as detected by HR-pQCT: a retrospective cross-sectional study

**Nicola Oehler[1] · Tim Rolvien[1] · Tobias Schmidt[1] · Sebastian Butscheidt[2] · Ralf Oheim[2] · Florian Barvencik[2] · Haider Mussawy[1]**

Received: 5 June 2018 / Accepted: 1 November 2018 / Published online: 21 November 2018


## Abstract

In the course of complex regional pain syndrome (CRPS), local osteopenia in the subchondral/subcortical areas of the affected limb represents a central manifestation. Mechanistic aspects of CRPS-associated pathologies remain unclear, and knowledge about bone morphology in CRPS-affected areas is rare. The aim of this study was to assess trabecular and cortical bone microstructure in patients with CRPS of the distal tibiae. We retrospectively analysed 14 women diagnosed with unilateral CRPS type I of the lower limb whose affected and unaffected distal tibiae were examined by high-resolution peripheral quantitative computed tomography (HR-pQCT). Laboratory tests included serum levels of calcium, phosphate, 25-hydroxyvitamin D, bone alkaline phosphatase, parathyroid hormone, osteocalcin and urinary levels of deoxypyridinoline (DPD). Bone mineral density was measured by dual-energy X-ray absorptiometry (DXA) at the lumbar spine and both proximal femurs. Average urinary DPD levels, a biochemical marker of bone resorption, were elevated in the examined patient cohort ($7.1 \pm 1.9$ nmol/mmol, reference 3.0–7.0 nmol/mmol). According to HR-pQCT, CRPS-affected distal tibiae showed significantly lower values of cortical BMD and cortical thickness compared to the unaffected contralateral side. Also, bone volume relative to total volume was significantly lower. Trabecular number and trabecular thickness tended to be lower in the affected tibiae. CRPS is associated with significant alterations in bone microstructure of the affected tibiae. Increased bone resorption seems to play a crucial role within a multifactorial process of CRPS-mediated bone atrophy. HR-pQCT could possibly serve as a diagnostic tool in specific CRPS therapy.

**Keywords** Complex regional pain syndrome · CRPS · Bone microstructure · HR-pQCT

## Introduction

Complex regional pain syndrome (CRPS) is a chronic neuropathic pain disorder mostly occurring in distal extremities after tissue trauma, which is characterised by disproportionate pain relative to duration or magnitude of injury [1]. It is classified as CRPS type I and II, depending on the presence or absence of direct peripheral nerve injuries [1, 2]. Diagnosis is based on the clinical symptoms according to the updated Budapest Criteria [3]. These clinical signs often exhibit a complex variety with characteristic occurrence in the course of the disease with allodynia, oedema, increased local temperature, sweating and altered pattern of hair/nail growth in the early phases, and a decrease of the local temperature in the later dystrophic phase [1, 4]. Another substantial finding is focal osteopenia in the subchondral and subcortical areas of the affected limb [5]. Pathogenetic mechanisms leading to these diverse manifestations are assumed to be multifactorial and based on the great variability of clinical presentations, the relative contributions of different mechanisms may vary across individual patients [1]. Local release of pro-inflammatory neuropeptides and cytokines followed by deranged capillary permeability with oedema, consequent hypoxia and acidosis are increasingly

**Electronic supplementary material** The online version of this article (https://doi.org/10.1007/s00774-018-0976-2) contains supplementary material, which is available to authorized users.

✉ Nicola Oehler
n.oehler@uke.de

[1] Department of Orthopaedic Surgery, University Medical Centre Hamburg-Eppendorf, Martinistraße 52, 20246 Hamburg, Germany

[2] Department of Osteology and Biomechanics, University Medical Centre Hamburg-Eppendorf, Lottestraße 59, 22529 Hamburg, Germany

accepted approaches to CRPS pathology [6]. Additionally, sympatho-afferent coupling and altered central nervous system signalling are also debated to be involved in pathogenesis [1]. Yet, despite extensive investigation in this field, the exact aetiology and pathophysiological pathways remain uncertain. As such, effects on histologic bone morphology in the course of CRPS-mediated bone atrophy are still poorly understood [7, 8]. In this context, HR-pQCT represents an excellent technology for detecting in vivo alterations of trabecular and cortical bone microstructure of peripheral bones including the distal tibia [9]. Thus, the aim of this retrospective study was to improve our comprehension of bone remodelling processes and of both trabecular and cortical microstructure in CRPS-affected patients using laboratory evaluations and HR-pQCT examinations of CRPS-affected distal tibiae compared to the unaffected contralateral sides in 14 female patients.

## Materials and methods

### Study group

In this study, we examined 14 consecutive women with CRPS of the lower limb who underwent HR-pQCT of both the affected and unaffected distal tibiae. Diagnosis was based on the clinical symptoms according to the updated Budapest Criteria [3]. This retrospective analysis was conducted in accordance with the principles of the Declaration of Helsinki and evaluated according to the rules of the local ethics committee of the University Medical Centre Hamburg-Eppendorf, Germany (protocol number WF-25/16).

### Laboratory assessment and dual-energy X-ray absorptiometry

Biochemical analyses of bone metabolism markers including serum levels of calcium, phosphate, 25-hydroxyvitamin D (25-OH-$D_3$), bone-specific alkaline phosphatase (BAP), parathyroid hormone (PTH), osteocalcin and urinary levels of deoxypyridinoline (DPD) were assessed by routine laboratory tests at the time of consultation. Reference values were adapted from the laboratory of the University Medical Centre Hamburg-Eppendorf for each parameter. BMD was measured by dual-energy X-ray absorptiometry (DXA, Lunar iDXA, GE Healthcare; Madison, WI, USA) at the lumbar spine and both proximal femurs. The detected BMD of the projected bone area was expressed in grams per square centimetre (g/$cm^2$), and the corresponding *T* and *Z* scores were calculated. The *T* score was used to determine normal BMD ($> -1.0$), osteopenia ($\leq -1.0$ and $> -2.5$) or osteoporosis ($\leq -2.5$) based on the World Health Organization (WHO) criteria for osteoporosis.

### HR-pQCT

The affected and unaffected tibiae were assessed by HR-pQCT (XtremeCT, SCANCO Medical, Brüttisellen, Switzerland). The default in vivo settings were applied, namely 60 kVp, 1000 µA, 100 ms integration time, and resolution of 82 µm. The measurement region was manually defined by a trained operator by placing a reference line at the endplate of the tibia on a preliminarily performed scout view. The same operator generates semiautomatic contours around the periosteal surface and the entire volume of interest is thereafter automatically separated into a cortical and trabecular region. Five different grades were manually defined by the same operator from grade 1 (no visible motion artefacts) to grade 5 (severe motion artefacts) [10]. According to the study by Pauchard et al., images should not exceed a manual grading of 3 [11]. A quality scan for calibration of the CT system was performed each day using a phantom provided by the manufacturer. The manufacturer's standard protocol was used to analyse the bone microstructure including bone volume to total volume ratio (BT/TV), trabecular number (Tb.N), trabecular thickness (Tb.Th), cortical thickness (Ct.Th) and cortical bone mineral density (Ct.BMD). HR-pQCT values are expressed as absolute values.

### Statistics

Statistical analysis was performed using GraphPad Prism 7 software. Continuous and categorical variables were expressed as mean ± standard deviation (range) and n, respectively. The affected and unaffected tibiae were compared in terms of mean BV/TV, Tb.N, Tb.Th, Ct.Th and Ct.BMD using paired Student's *t* test. Correlation between disease duration and changes of the parameters of HR-pQCT was analysed using Spearman coefficient. $p$ values $< 0.05$ were considered statistically significant.

## Results

### Patient characteristics and biochemical bone turnover results

Of the examined cohort, all 14 patients were female. Mean age was 50.0 ± 13.9 (range 18–65) years and both right and left tibiae were equally affected (left/right = 7/7, Table 1). Six patients developed CRPS after direct trauma of the ankle/tarsal bones or supination trauma of the upper ankle with bone marrow oedema or ligamentous lesions. Four patients had been diagnosed with stress fractures of the ankle/tarsal bones and one each with fracture of the femur,

**Table 1** Diagnostic characteristics of patients with CRPS ($n=14$)

| Patient number | Gender (m/f) | Side affected (left/right) | Age (years) | DXA | | | | | Laboratory data | | | | | | |
|---|---|---|---|---|---|---|---|---|---|---|---|---|---|---|---|
| | | | | Z score (lumbar spine) | Z score (affected total hip) | Z score (unaffected total hip) | Z score (affected femoral neck) | Z score (unaffected femoral neck) | Calcium (mmol/l) | Phosphate (mmol/l) | 25-OH-$D_3$ (µg/l) | PTH (ng/l) | DPD (nmol/mmol) | Bone AP (µg/l) | Osteocalcin (µg/l) |
| 1 | f | Left | 35 | −1.1 | −0.8 | −1.1 | −0.5 | −0.8 | 2.28 | 1.02 | 16.7 | 22.4 | 6.0 | 6.6 | 14.0 |
| 2 | f | Right | 51 | −0.9 | – | −0.5* | – | −0.2* | 2.16 | 0.78 | 25.4 | 112.4 | 12.0 | 10.9 | 19.4 |
| 3 | f | Left | 34 | 0.4 | −0.3 | 0.4 | −0.3 | 0.4 | 2.26 | 0.85 | 45.6 | 27.7 | 7.0 | 6.4 | 18.1 |
| 4 | f | Right | 62 | 0.2 | −0.2 | 0.3 | −0.2 | 0.4 | 2.32 | 1.11 | 28.2 | 82.7 | 9.0 | 12.5 | 19.6 |
| 5 | f | Right | 48 | −0.4 | −0.8 | −1.1 | −0.5 | −0.8 | 2.24 | 0.97 | 21.8 | 58.2 | 6.0 | 14.9 | 18.7 |
| 6 | f | Right | 57 | −2.4 | −1.3 | −1.0 | −1.0 | −0.8 | 2.49 | 1.08 | 35.4 | 67.8 | 7.0 | 14.7 | 25.2 |
| 7 | f | Right | 52 | 0.3 | 0.7 | 0.4 | 1.0 | 0.4 | 2.31 | 1.18 | 20.36 | 60.8 | 6.0 | 12.8 | 19.7 |
| 8 | f | Left | 65 | −2.4 | −1.9 | −1.5 | −0.9 | −0.7 | 2.31 | 0.99 | 26.1 | 34.7 | 7.0 | 14.1 | 12.8 |
| 9 | f | Left | 38 | 0.7 | −0.9 | −1.1 | −0.7 | −1.0 | 2.23 | 1.15 | 20.9 | 36.8 | 7.0 | 5.4 | 20.7 |
| 10 | f | Right | 18 | −0.6 | −0.6 | −0.5 | −0.1 | −0.1 | 2.15 | 1.07 | 14.36 | 71.8 | 7.0 | 15.9 | 16.8 |
| 11 | f | Left | 59 | −0.3 | 0.4* | – | 0.5* | – | 2.22 | 0.80 | 14.7 | 41.4 | 9.0 | 41.5 | 18.3 |
| 12 | f | Left | 57 | −0.2 | −2.1 | −1.8 | −1.5 | −1.4 | 2.30 | 1.08 | 26.2 | 73.2 | 6.0 | 9.8 | 18.9 |
| 13 | f | Left | 65 | −1.2 | −1.7 | −1.7 | 0.9 | −0.5 | 2.42 | 0.99 | 24.9 | 32.8 | 4.0 | 13.7 | 12.2 |
| 14 | f | Right | 59 | −1.0 | −0.1 | −1.0 | −0.1 | −0.4 | 2.29 | 1.19 | 27.8 | 63.6 | 7.0 | 22.2 | 20.4 |
| Mean ± SD | | | 50.0 ± 13.9 | −0.64 ± 0.95 | −0.83 ± 0.82 | −0.81 ± 0.79 | −0.33 ± 0.72 | −0.44 ± 0.60 | 2.28 ± 0.09 | 1.02 ± 0.13 | 24.9 ± 8.3 | 56.2 ± 25.1 | 7.1 ± 1.9 | 14.4 ± 9.0 | 18.2 ± 3.4 |
| Reference values | | | | | | | | | 2.13–2.63 | 0.77–1.50 | 30.0–60.0 | 17.0–84.0 | 3.0–7.0 | 5.2–24.4 | 5.4–59.1 |

Demographic data, mean values of laboratory results and bone mineral density measured by DXA are shown. Dual-energy X-ray absorptiometry (DXA); 25-hydroxyvitamin D (25-OH-$D_3$); deoxypyridinoline (DPD); parathyroid hormone (PTH); bone alkaline phosphatase (BAP)

*Excluded from calculation of mean values

rupture of the ACL, and with empyema of the upper ankle joint. One patient developed CRPS after undergoing ankle joint prosthesis implantation. One patient, who was diagnosed with bone marrow oedema without a fracture, showed the pathology directly within the examined area of the distal tibia. Imaging of the affected lower limb including radiography was conducted and revealed focal osteopenia within the tarsal bones (Fig. 1a, b). PD-weighted MRI indicates diffuse bone marrow oedema in the distal tibia and talus (Fig. 1c). Average values of laboratory examinations of calcium (2.28 ± 0.09 mmol/l), phosphate (1.02 ± 0.13 mmol/l), 25-OH-$D_3$ (24.9 ± 8.3 µg/l), PTH (56.2 ± 25.1 ng/l), bone AP (14.4 ± 9.0 µg/l) and osteocalcin (18.2 ± 3.4 µg/l) were within the normal range (Table 1). Notably, urinary levels of DPD, an appropriate biochemical marker of bone resorption were elevated or at the upper reference limit in nine patients with a mean level of 7.1 ± 1.9 nmol/mmol, thus exceeding the reference range (reference 3.0–7.0 nmol/mmol, Table 1 and Fig. 2). Of all the examined patients, five with fractures unloaded the affected extremity for 6 weeks and one after undergoing ankle joint prosthesis implantation for 2 weeks according to our records. Time period after the phase of unloading time until HR-pQCT examination was 1–7 months in four patients ranging up to 14 and 116 months in the other two cases, respectively. The remaining patients could bear (at least pain-adapted) full body weight.


**Fig. 1** Imaging findings in CRPS. **a**, **b** Radiographs of the right ankle of a patient with CRPS showing focal osteopenia within the tarsal bones. Red box indicates the scanning volume for HR-pQCT analysis. **c** PD-weighted MRI indicates diffuse bone marrow oedema in the distal tibia and talus

## Bone mineral density (DXA) and bone microstructure (HR-pQCT)

According to the measured *T* scores of DXA examination, six patients were diagnosed with osteopenia and four with osteoporosis. The calculation of *Z* scores of all the examined patients resulted in a mean of − 0.64 ± 0.95 at the lumbar spine and − 0.85 ± 0.76 and − 0.67 ± 0.84 for the left and the right total femur and − 0.35 ± 0.67 and − 0.41 ± 0.66 for the left and right femoral neck, respectively. Of note, comparison of BMD according to *Z* scores of the affected and the unaffected total femur and femoral neck did not display significant differences (total femur − 0.83 ± 0.82 vs. − 0.81 ± 0.79, $p = 0.85$; femoral neck − 0.33 ± 0.72 vs. − 0.44 ± 0.60, $p = 0.49$; Table 1). All 14 patients underwent

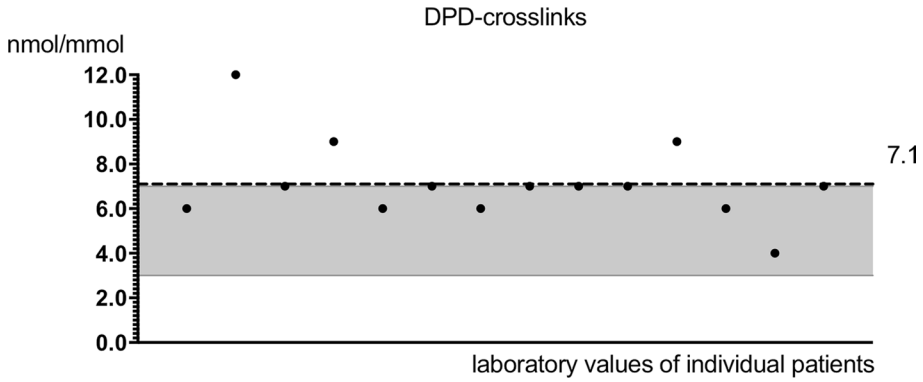


**Fig. 2** Laboratory values of DPD (reference 3.0–7.0 nmol/mmol) of patients with CRPS. Dots show individual values of each patient. Dashed line shows mean of all patients. Area shaded grey represents reference range

HR-pQCT examination of both the affected and unaffected distal tibiae. The mean disease duration from CRPS diagnosis to HR-pQCT was 10.1 (range 0–111) months. Notably, the affected tibiae displayed significantly lower values of cortical BMD (Ct.BMD 741.2 ± 70.3 vs. 775.3 ± 69.4 mg HA/ccm, $p = 0.0011$, Fig. 3a) and cortical thickness (Ct.Th 0.72 ± 0.25 vs. 0.81 ± 0.24 mm, $p = 0.0068$, Fig. 3b) in pairwise comparisons. Also, distal tibiae with CRPS were found to show significantly lower bone volume per tissue volume (BV/TV 0.10 ± 0.02 vs. 0.11 ± 0.03, $p = 0.05$, Fig. 3c). Trabecular number and trabecular thickness were not different between the affected and unaffected sides (Tb.N 1.72 ± 0.31 vs. 1.76 ± 0.40 1/mm, $p = 0.52$; Tb.Th: 0.061 ± 0.008 vs. 0.063 ± 0.006 mm, $p = 0.34$, Fig. 3d, e). Figure 4a–d shows high-resolution quantitative computed tomography images of the affected and unaffected tibiae of one patient. The analysis of the relation between disease duration and the extent of alterations of both cortical and trabecular microstructures did not show any significant correlation (Supplementary Table 1).

## Discussion

This retrospective study on patients with unilateral CRPS of the lower limb demonstrates substantial alterations in bone microstructure in HR-pQCT scans of the affected distal tibia in comparison to the unaffected contralateral side. This was

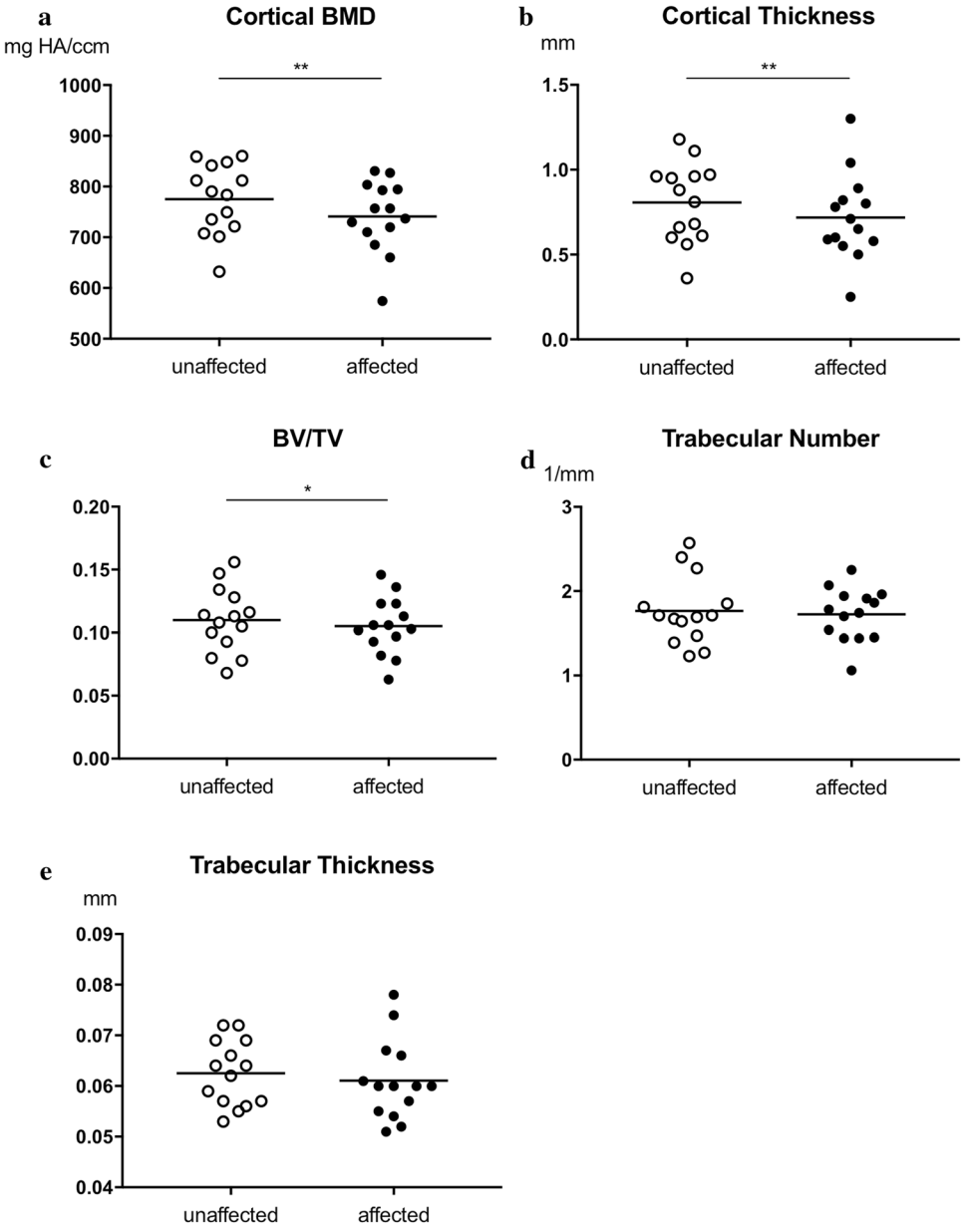


**Fig. 3** Cortical and trabecular bone microstructure measured by HR-pQCT in CRPS-affected distal tibiae in pairwise comparison to the unaffected contralateral side. **a** Cortical bone mineral density (Ct.BMD), **b** cortical thickness (Ct.Th), **c** bone volume to total volume ratio (BT/TV), **d** trabecular number (Tb.N) and **e** trabecular thickness (Tb.Th). Black circles show values of CRPS-affected tibiae, white circles show unaffected contralateral tibiae. All values are absolute mean ± standard deviation (*$p < 0.05$, **$p < 0.01$ as determined by paired Student's *t* test)

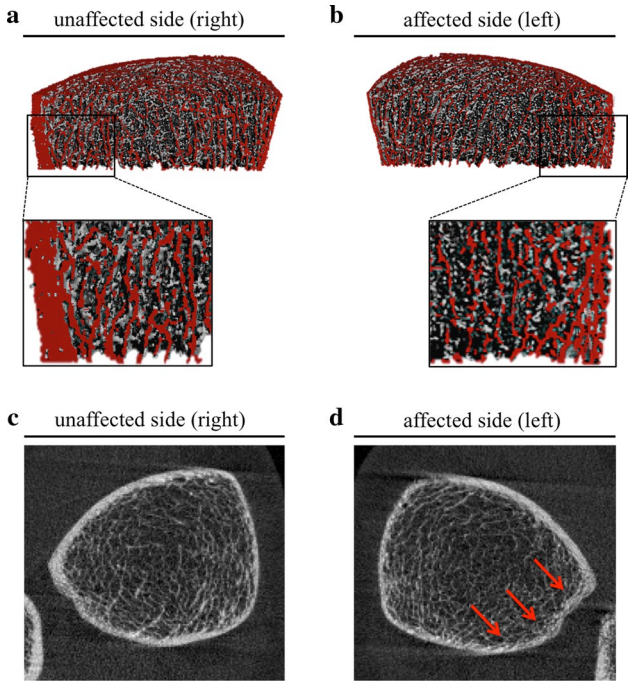


**Fig. 4** Bilateral HR-pQCT scans of the distal tibiae of a patient with CRPS. **a**, **b** 3D reconstructions of the unaffected and affected sides. **c**, **d** Single layer from HR-pQCT. Red arrows indicate the cortical deterioration at the left distal tibia

expressed by significantly lower cortical BMD, cortical thickness and bone volume per tissue volume. Furthermore, biochemical evidence for increased bone resorption with an elevation of urinary DPD levels could be detected.

Focal bone loss represents one central element in CRPS pathology and is characterised by irregular demineralisation with patchy atrophic appearance on X-rays [2, 12] and a local reduction of bone mineral density within the affected limbs [13]. Yet, detailed morphologic information is still rare. In our study, parameters of the cortical structure were clearly reduced in the affected tibiae compared to the unaffected contralateral side. Alterations of the trabecular number and thickness did not reach significance. However, BV/TV, a parameter that is derived from trabecular BMD and trabecular number, was significantly reduced between the affected and unaffected sides.

Our findings are consistent with a recent report, which demonstrated a decrease in both trabecular and cortical volumetric bone mineral density and cortical thickness within the CRPS-affected tibia analysed by qCT [12]. In a previous study of our group on CRPS-mediated alterations of bone microstructure in the upper extremity, only the trabecular structures were found to be affected [14]. The differences in bone alterations may be due to the fact that 60% of the patients in our first study had a previous wrist fracture, which is in the area of interest where the measurement with HR-pQCT was performed. Likewise, Wang et al. also showed trabeculae of CRPS-affected tibiae in a rat model to be exclusively altered in a µCT analysis [15]. However, fractures within the examined area were the prevailing cause of the CRPS pathology. This may influence the cortical bone and may even prevent cortical deterioration or increase cortical thickness due to fracture healing processes. In the present cohort by contrast, no patient had been diagnosed with a fracture directly within the distal tibia.

The detected morphologic alterations may to some extent be attributable to disuse of the affected limb. Indeed, bone loss following disuse has been postulated by DXA analysis of both proximal femurs to lead to a reduction of BMD within the affected limb as compared to the unaffected side [16]. Also, HR-pQCT analyses revealed alterations in primarily cortical bone structures [16, 17]. Yet, first, comparison of the femoral BMD according to DXA in our patient cohort did not reveal any differences. Second, in the latter study, neither cortical BMD nor BV/TV was significantly altered compared to the contralateral limb, and trabecular number was even slightly elevated [17]. Most importantly, 10/14 patients in our study could bear full body weight on the affected limb at the time of examination, all of which make disuse-induced atrophy unlikely and emphasise the present microstructural alterations to be predominantly mediated by CRPS pathology.

Surprisingly, although laboratory examinations in patients with CRPS have so far not revealed characteristic profiles [8, 12, 18], we found the average urinary levels of DPD to be elevated. DPD is a product of collagen degradation [19] and thus indicates that the increased bone resorption might play a central role in the detected CRPS-mediated bone atrophy. Wang et al. recently demonstrated promotion of osteoclastic activity as a potential pathogenetic mechanism in histomorphometric analyses of CRPS-affected tibiae of rats [15]. Besides, bisphosphonates as potent inhibitors of osteoclastic activity have been proven to exert beneficial effects in the course of CRPS disease in terms of pain, mobility and bone loss [5, 13, 20]. The scintigraphically detectable high bone turnover in CRPS [21] also indirectly favours this pathogenetic approach. Yet, exact osteoclastogenic pathways remain controversial. While pathological sympatho-afferent coupling and central dysregulation are long debated as pathogenetic aspects of CRPS [22], bone metabolism is also known to be regulated centrally, mediated by the sympathetic nervous system and neuroendocrine mechanisms [23]. Since osteoblasts are equipped with adrenergic receptors and stimulation of the sympathetic nervous system has been demonstrated to not only hinder osteoblastic bone formation but also to induce osteoclastogenesis via activation of NF-κB ligand (RANKL) [24], bone loss in CRPS patients may thus be attributable to this assumed sympathetic and

central dysfunction. Additionally, facilitated neurogenic inflammation is increasingly being discussed as another pathogenetic approach with the enhanced release of neuropeptides and cytokines [6], of which both substance *P* and cytokines such as TNFα are postulated to promote osteoclastic activity [22, 25, 26]. These neuroinflammatory substances and cytokines also induce dysregulation of capillary exchange, oedema, local hypoxia and local acidosis, which have been proposed to possibly lead to the chemical dissolution of hydroxyapatite crystals thus promoting bone atrophy [5, 6, 18]. Also, with the detection of elevated osteoprotegerin levels in CRPS-affected patients and the hypothesis of an impaired vitamin K-dependent carboxylation of osteocalcin (a biochemical marker of bone formation) in CRPS disease, perturbation of osteoblastic activity has been suggested as another potential mechanism [27, 28]. Thus, increased bone resorption with an activation of osteoclastic activity might represent one aspect integrated in a multifactorial process driving bone atrophy in CRPS disease.

There are certainly considerable limitations to the present study. First, the retrospective study design does not only prohibit follow-up examinations of the patients, but also restricts the ability to draw any causal conclusions. Second, since the major subset of our patient cohort underwent HR-pQCT within a short period after primary diagnosis of CRPS, the validity of analyses with regard to the time course of the disease remains limited. Third, a number of women were in the menopause, which could have, amongst other factors, influenced bone remodelling parameters and especially bone resorption markers. Fourth, the measurement was done by the first-generation HR-pQCT and may not accurately depict the crossing between cortical and trabecular compartments. Measurements with better resolution, at least second-generation HR-pQCT, are recommended. However, since our results represent the first approach of understanding the skeletal status of patients with CRPS including bone turnover markers, future studies (e.g. with control groups) are needed to confirm the presence of high bone resorption markers in CRPS.

In summary, we could demonstrate substantial microstructural alterations of cortical and trabecular bone tissues in CRPS-affected tibiae and thus provide new insight into the morphological and pathophysiological bone-specific processes caused by CRPS. Since bisphosphonates represent an increasingly accepted therapeutic approach for this disease, it is tempting to speculate that microstructural analyses could possibly serve as a useful tool for identifying those patients who could benefit from bisphosphonate treatment.

**Acknowledgements** The authors thank Felix N. Schmidt for his excellent assistance with the HR-pQCT imaging.

## Compliance with ethical standards

**Conflict of interest** All authors have no conflict of interest.

**Ethical approval** All procedures performed in studies involving human participants were in accordance with the ethical standards of the institutional and/or national research committee and with the 1964 Helsinki declaration and its later amendments or comparable ethical standards.

## References

1. Bruehl S (2015) Complex regional pain syndrome. BMJ 351:h2730
2. Gatti D, Rossini M, Adami S (2016) Management of patients with complex regional pain syndrome type I. Osteoporos Int 27:2423–2431
3. Harden RN, Bruehl S, Perez RS, Birklein F, Marinus J, Maihofner C, Lubenow T, Buvanendran A, Mackey S, Graciosa J, Mogilevski M, Ramsden C, Chont M, Vatine JJ (2010) Validation of proposed diagnostic criteria (the "Budapest Criteria") for complex regional pain syndrome. Pain 150:268–274
4. Wei T, Guo TZ, Li WW, Kingery WS, Clark JD (2016) Acute versus chronic phase mechanisms in a rat model of CRPS. J Neuroinflammation 13:14
5. Giusti A, Bianchi G (2015) Treatment of complex regional pain syndrome type I with bisphosphonates. RMD Open 1:e000056
6. Varenna M, Zucchi F (2015) Algodystrophy: recent insight into the pathogenic framework. Clin Cases Miner Bone Metab 12:27–30
7. Basle MF, Rebel A, Renier JC (1983) Bone tissue in reflex sympathetic dystrophy syndrome–Sudeck's atrophy: structural and ultrastructural studies. Metab Bone Dis Relat Res 4:305–311
8. Renier JC, Basle M, Arlet J, Seret P, Acquaviva P, Schiano A, Roux C, Serratrice G, Amor B, May V, Ryckewaert A, Delcambre B, d'Eshougues R, Vincent G, Ducastelle, Desproges Gotteron R, Le Goff P, Gougeon J, Hautin et al (1983) Bone and phosphorocalcium metabolism in reflex sympathetic dystrophy. Rev Rhum Mal Osteoartic, 50:23–31
9. Cheung AM, Adachi JD, Hanley DA, Kendler DL, Davison KS, Josse R, Brown JP, Ste-Marie LG, Kremer R, Erlandson MC, Dian L, Burghardt AJ, Boyd SK (2013) High-resolution peripheral quantitative computed tomography for the assessment of bone strength and structure: a review by the Canadian Bone Strength Working Group. Curr Osteoporos Rep 11:136–146
10. Pialat JB, Burghardt AJ, Sode M, Link TM, Majumdar S (2012) Visual grading of motion induced image degradation in high resolution peripheral computed tomography: impact of image quality on measures of bone density and micro-architecture. Bone 50:111–118
11. Pauchard Y, Liphardt AM, Macdonald HM, Hanley DA, Boyd SK (2012) Quality control for bone quality parameters affected by subject motion in high-resolution peripheral quantitative computed tomography. Bone 50:1304–1310
12. Simm PJ, Briody J, McQuade M, Munns CF (2010) The successful use of pamidronate in an 11-year-old girl with complex regional pain syndrome: response to treatment demonstrated by serial peripheral quantitative computerised tomographic scans. Bone 46:885–888
13. Adami S, Fossaluzza V, Gatti D, Fracassi E, Braga V (1997) Bisphosphonate therapy of reflex sympathetic dystrophy syndrome. Ann Rheum Dis 56:201–204

14. Mussawy H, Schmidt T, Rolvien T, Ruther W, Amling M (2017) Evaluation of bone microstructure in CRPS-affected upper limbs by HR-pQCT. Clin Cases Miner Bone Metab 14:54–59
15. Wang L, Guo TZ, Wei T, Li WW, Shi X, Clark JD, Kingery WS (2016) Bisphosphonates inhibit pain, bone loss, and inflammation in a rat tibia fracture model of complex regional pain syndrome. Anesth Analg 123:1033–1045
16. del Puente A, Pappone N, Mandes MG, Mantova D, Scarpa R, Oriente P (1996) Determinants of bone mineral density in immobilization: a study on hemiplegic patients. Osteoporos Int 6:50–54
17. Kazakia GJ, Tjong W, Nirody JA, Burghardt AJ, Carballido-Gamio J, Patsch JM, Link T, Feeley BT, Ma CB (2014) The influence of disuse on bone microstructure and mechanics assessed by HR-pQCT. Bone 63:132–140
18. Varenna M (2014) Bisphosphonates beyond their anti-osteoclastic properties. Rheumatol (Oxf) 53:965–967
19. Robins SP, Duncan A, Wilson N, Evans BJ (1996) Standardization of pyridinium crosslinks, pyridinoline and deoxypyridinoline, for use as biochemical markers of collagen degradation. Clin Chem 42:1621–1626
20. Chevreau M, Romand X, Gaudin P, Juvin R, Baillet A (2017) Bisphosphonates for treatment of complex regional pain syndrome type 1: a systematic literature review and meta-analysis of randomized controlled trials versus placebo. Joint Bone Spine 84:393–399
21. Nitzsche EU (2011) Nuclear medicine imaging for diagnosis of CRPS I. Handchir Mikrochir Plast Chir 43:20–24
22. Maihofner C, Seifert F, Markovic K (2010) Complex regional pain syndromes: new pathophysiological concepts and therapies. Eur J Neurol 17:649–660
23. Amling M, Takeda S, Karsenty G (2000) A neuro (endo)crine regulation of bone remodeling. BioEssays 22:970–975
24. Elefteriou F, Ahn JD, Takeda S, Starbuck M, Yang X, Liu X, Kondo H, Richards WG, Bannon TW, Noda M, Clement K, Vaisse C, Karsenty G (2005) Leptin regulation of bone resorption by the sympathetic nervous system and CART. Nature 434:514–520
25. Goto T, Tanaka T (2002) Tachykinins and tachykinin receptors in bone. Microsc Res Tech 58:91–97
26. Kitaura H, Kimura K, Ishida M, Kohara H, Yoshimatsu M, Takano-Yamamoto T (2013) Immunological reaction in TNF-alpha-mediated osteoclast formation and bone resorption in vitro and in vivo. Clin Dev Immunol 2013:181849
27. Ediz L, Hiz O, Meral I, Alpayci M (2010) Complex regional pain syndrome: a vitamin K dependent entity? Med Hypotheses 75:319–323
28. Kramer HH, Hofbauer LC, Szalay G, Breimhorst M, Eberle T, Zieschang K, Rauner M, Schlereth T, Schreckenberger M, Birklein F (2014) Osteoprotegerin: a new biomarker for impaired bone metabolism in complex regional pain syndrome? Pain 155:889–895